

Benefits of Cruise Design Optimization for High-Performance, Single-Engine Airplanes

Bruce J. Holmes*

NASA Langley Research Center, Hampton, Va.

A design study has been conducted to optimize a single-engine airplane for a high-performance cruise mission. The mission analyzed included a cruise speed of 300 knots, a cruise range of 1300 n.mi., and a six-passenger payload [5340 N (1200 lb), including crew]. The purpose of the study is to evaluate the practicality of combinations of wing design, cruise power, and operating altitude required for the mission. The results show that these ambitious mission performance characteristics can be achieved with fuel efficiencies competitive with present-day high-performance, single- and twin-engine business airplanes. It is noted that relaxation of the present Federal Aviation Regulation, Part 23, stall-speed requirement for single-engine airplanes facilitates the optimization of the airplane for cruise fuel efficiency.

Nomenclature†

A	= aspect ratio = $b^2 S^{-1}$
b	= wing span, m (ft)
B	= Breguet factor, n.mi.
c	= specific fuel consumption, $\text{kg} \cdot \text{kW}^{-1} \cdot \text{h}^{-1}$ ($\text{lb} \cdot \text{hp}^{-1} \cdot \text{h}^{-1}$)
$C_{L_{cr}}$	= cruise lift coefficient
C_{L_m}	= lift coefficient at $(L/D)_m$
C_{D_0}	= airplane zero-lift-drag coefficient
$C_{D_{\pi, \text{wing}}}$	= wing zero-lift-drag coefficient
$C_{L_{\text{max}}}$	= maximum airplane lift coefficient
e	= Oswald's (airplane) efficiency factor
$f_{\pi_{\text{fus}}}$	= fuselage + tail equivalent flat plate area, m^2 (ft^2)
h_{cr}	= cruise altitude, m (ft)
K_1	= gross weight factor
K_2	= propulsion system specific weight, N/kW (lb/hp)
K_3	= Breguet equation constant, $198.2 \text{ kg} \cdot \text{n.mi.} \cdot \text{kW}^{-1} \cdot \text{h}^{-1}$ ($325.9 \text{ lb} \cdot \text{n.mi.} \cdot \text{hp}^{-1} \cdot \text{h}^{-1}$)
K_4	= engine lapse rate, P_{sl}/P_{alt}
K_5	= constant, $17.24 \text{ kg}^{-1} \cdot \text{m}^3$ ($9.5 \text{ slugs}^{-1} \cdot \text{ft}^3$)
$(L/D)_{cr}$	= lift-to-drag ratio at V_{cr}
$(L/D)_m$	= maximum lift-to-drag ratio
n	= design cruise lift coefficient ratio = $C_{L_{cr}}/C_{L_m}$
P_{cr}	= cruise thrust power required at V_{cr} , kW (hp)
P_m	= thrust power required at V_m , kW (hp)
P_{sl}	= sea-level installed brake power, kW (hp)
R_{cr}	= cruise range at V_{cr} , n.mi.
R_m	= maximum range at V_m , n.mi.
S	= reference planform wing area, m^2 (ft^2)
\bar{U}	= useful load fraction = $1 - W_e/W$
V_{cr}	= cruise true airspeed, knots
V_m	= true airspeed at $(L/D)_m$, knots
V_{s0}	= stall speed in landing configuration, knots
W	= airplane gross weight, N (lb)

W_e	= airplane empty weight, N (lb)
W_f	= fuel weight, N (lb)
W_p	= payload, N (lb)
W_t	= propulsion system weight, N (lb)
W/S	= wing loading, $\text{N} \cdot \text{m}^{-2}$ ($\text{lb} \cdot \text{ft}^{-2}$)
η_p	= propulsive efficiency
ρ_0	= air density, standard atmosphere at sea level, $\text{N} \cdot \text{m}^{-3}$ ($\text{slugs} \cdot \text{ft}^{-3}$)
ρ_{cr}	= air density at cruise altitude, $\text{N} \cdot \text{m}^{-3}$ ($\text{slugs} \cdot \text{ft}^{-3}$)
σ	= air density ratio = ρ_{cr}/ρ_0

Introduction

IN the nearly five decades since the introduction of general aviation airplanes used for business and private transportation, cruise speeds, ranges, and payloads have improved significantly. As Fig. 1 illustrates, increasing speeds and ranges have been achieved through the design of multiengine piston- and turbine-powered airplanes. This paper illustrates the potential for significant improvements in the mission performance of the high-performance, single-engine airplane. The analysis procedure and tradeoff data for this class of airplane are presented.

The mission selected for analysis (see Fig. 1) is cruise speed $V_{cr} = 300$ knots, cruise range $R_{cr} = 1300$ n.mi. (no reserves), and payload $W_p = 5338$ N (1200 lb or six passengers with baggage, including crew). These performance objectives are significant in that they represent approximately a 100% increase in cruise speed and in range (at maximum cruise speed) over current single-engine business airplanes. This single-engine mission performance is comparable to that for current high-performance, twin-engine, turboprop airplanes.

Typically, in general aviation airplane design, cruise speed V_{cr} is much greater than the speed where maximum lift-to-drag ratio occurs, V_m ; hence cruise lift-to-drag ratio $(L/D)_{cr}$ is much less than the maximum lift-to-drag ratio $(L/D)_m$ for current airplanes. This fact results from constraints placed on wing loading by current design practices and by Federal Aviation Regulations (FAR's). In current practice, wing loading is constrained by present high-lift system design practice coupled with FAR Paragraph 23.49, which states that " V_{s0} at maximum weight may not exceed 61 knots for single-engine airplanes" For this study, wing loading is assumed to be unconstrained by these current limitations in order to analyze what design benefits accrue to higher values of wing loading. These higher wing loadings permit V_m to increase in a fashion which produces a closer match between V_m and cruise speed. Then $(L/D)_{cr}$ occurs closer to $(L/D)_m$

Presented as Paper 80-1846 at the AIAA Aircraft Systems and Technology Meeting, Anaheim, Calif., Aug. 4-6, 1980; submitted Sept. 11, 1980; revision received Aug. 13, 1981. This paper is declared a work of the U.S. Government and therefore is in the public domain.

*Aerospace Technologist, Subsonic Aerodynamics Branch, Low-Speed Aerodynamics Division.

†Except for airspeed, which is given in knots (1 knot = 0.514 m/s), data are presented in the International System of Units (SI) with the equivalent values given parenthetically in U.S. Customary Units. The measurements and calculations were made in U.S. Customary Units. (Factors relating the two systems of units in this paper may be found in Ref. 1.)

Table 1 High-performance, single-engine airplane design parameters

Parameter	Value or range
Cruise speed V_{cr}	300 knots
Cruise range R_{cr}	1300 n.mi.
Cruise payload (including crew) W_p	5338 N (1200 lb)
Wing loading W/S	960-2900 N·m ⁻² (20-60 lb·ft ⁻²)
Design cruise lift coefficient ratio $C_{L_{cr}}/C_{L_m}$	0.4-0.9
Oswald's (airplane) efficiency factor	0.8
Maximum lift-to-drag ratio $(L/D)_m$	14-18
Engine	Scaled Pratt and Whitney PT6-A45A
Cruise specific fuel consumption c	0.334 kg·kW ⁻¹ ·h ⁻¹ (0.55 lb·hp ⁻¹ ·h ⁻¹)
Cruise propulsive efficiency η_p	0.85
Propulsion system specific weight K_2	3.88 N/kW (0.65 lb/hp)
Fuselage + tail equivalent flat plate area, $f_{\pi fus}$	0.159 m ² (1.71 ft ²)
Wing profile drag coefficient $C_{D_{\pi, wing}}$	0.0080

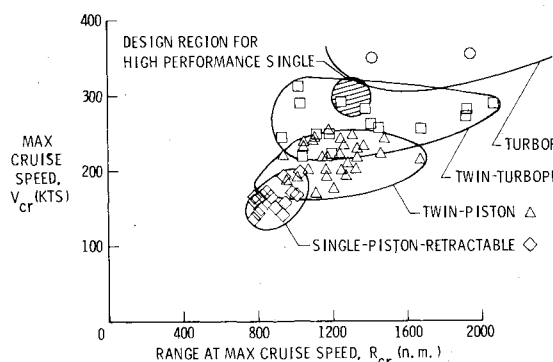
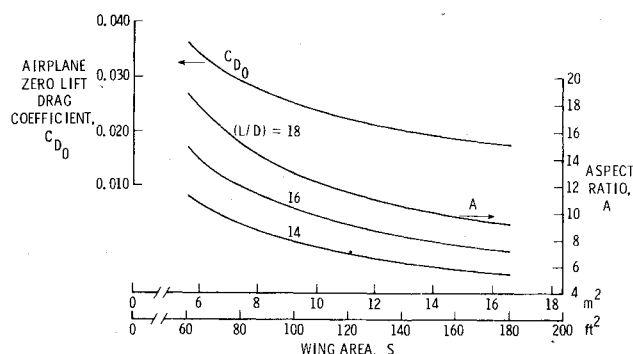


Fig. 1 Comparison of high-performance, single-engine airplane performance goal with current production airplane performance.

Fig. 2 Variation with wing area of total airplane profile drag and aspect ratio for given values of $(L/D)_m$, $f_{\pi fus} = 0.159 \text{ m}^2 (1.71 \text{ ft}^2)$.

and cruise fuel efficiency should improve. The design approach for this study involves varying wing geometry on a fixed fuselage design. The term "cruise-matched" is used herein to denote the relationship between design wing loading, power loading, and the ratios $(L/D)_{cr}/(L/D)_m$ and V_{cr}/V_m .

Design Data and Method

Design Data

The design parameters defined for this analysis are listed in Table 1. Several simplifying assumptions are made to facilitate the calculations. These assumptions are justified on the basis that they are consistent with the level of accuracy of the classical aerodynamic equations and empirical structural relationships used in this airplane sizing method.

Only the cruise segment of the flight is analyzed. No design constraints are imposed by taxi, takeoff, climb, or descent segments of the mission. This approach is reasonable, since it can be shown that engines which meet the cruise design requirements for airplanes resulting from this study could be flat-rated to meet typical general aviation field length requirements. Oswald's airplane efficiency factor e is assumed to be constant with changing aspect ratio. The effects of speed and altitude on specific fuel consumption c and on cruise propulsive efficiency η_p are ignored. While these effects might easily be accounted for, such precision of airplane sizing is not warranted for the results sought in this analysis.

The fuselage size is held constant, and is sized to carry six passengers with consideration given to pressurization requirements. The interior cabin width (outside elbow to outside elbow) is 122 cm (48 in.). Equivalent flat-plate area of the fuselage and tail were determined by the method of Ref. 2. A turboprop engine installation was assumed and account made for oil cooling drag. The wing profile drag coefficient was estimated by the method of Ref. 2, assuming fully turbulent boundary-layer drag. Then, for this constant-sized

fuselage and varying wing area, airplane zero-lift drag can be determined from the relation depicted in Fig. 2:

$$C_{D_0} = f_{\pi fus}/S + C_{D_{\pi, wing}} \quad (1)$$

where

$$f_{\pi fus} = 0.159 \text{ m}^2 (1.71 \text{ ft}^2)$$

and

$$C_{D_{\pi, wing}} = 0.0080$$

Empirical relations are used to determine airplane and component weights. A crude relation between propulsion system, payload, and fuel weights and the gross weight of the airplane may be written

$$W_t + W_p + W_f = K_1 W \quad (2)$$

where from Ref. 3, $K_1 = 0.60$. This value is based on an evaluation of the weight relationships for many production airplanes. The empirical relation between propulsion system size and weight was determined by analyzing several current production turboprop engines in the 750-kW power class and several high activity factor (4 bladed) propellers. A value of the propulsion system specific weight $K_2 = 3.88 \text{ N/kW}$ (0.65 lb/hp) resulted. Holding both of these weight relation factors (K_1 and K_2) constant can be considered a reasonable approximation for the purposes of this sizing study.

The engine power lapse rate (K_4) for the Pratt and Whitney PT6-A45A turboprop engine is used for any engine size resulting from the airplane sizing study. In addition, the lapse rate and specific fuel consumption for this engine were extrapolated beyond the 10,000-m limit of manufacturers data to about 14,000 m. The engine lapse rate characteristics are illustrated in Fig. 3.

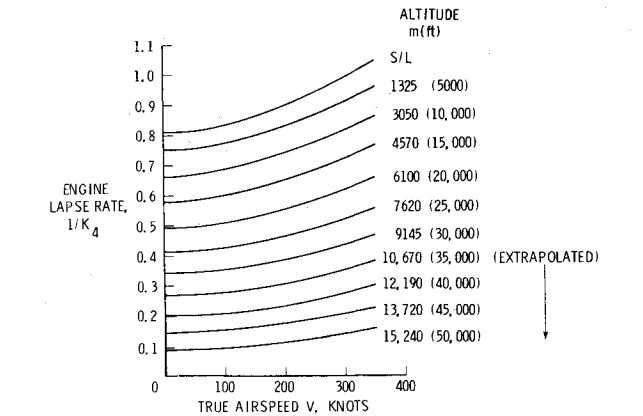


Fig. 3 Power characteristics of a Pratt and Whitney PT 6-A45A turboprop engine.

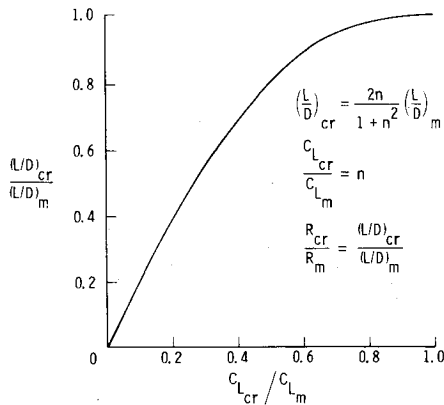


Fig. 4 The variation of the cruise L/D ratio with cruise lift-coefficient ratio.

A constant value of specific fuel consumption of $c=0.344$ kg/kW·h (0.55 lb/hp·h) is assumed. This value is used for $V_{cr}=300$ knots, with a maximum cruise throttle setting, for the range of altitudes which result from the analysis.

Aspect ratio is not defined, but rather computed based on the value of $(L/D)_m$, which is specified for the cases analyzed. Values for $(L/D)_m$ are varied between 14 and 18. For a parabolic drag polar, symmetrical about $C_L=0$, maximum lift-to-drag ratio is given by

$$(L/D)_m = \frac{1}{2} \sqrt{\frac{\pi A e}{C_{D0}}} \tag{3}$$

Thus for each value of $(L/D)_m$ specified in the design study, the combinations of C_{D0} and aspect ratio required to achieve the defined $(L/D)_m$ can be determined and are illustrated in Fig. 2.

In addition to specifying $(L/D)_m$, the proximity of the cruise lift coefficient C_{Lcr} to the lift coefficient for maximum lift-to-drag ratio, C_{Lm} , is defined. Thus cruise conditions are defined in the study by specifying n in the following relation:

$$C_{Lcr} = n C_{Lm} \tag{4}$$

For the parabolic, symmetric drag polar assumption, the following relation exists between cruise and maximum lift-to-drag ratios

$$(L/D)_{cr} = [2n / (1 + n^2)] (L/D)_m \tag{5}$$

The relation between Eqs. (4) and (5) is depicted in Fig. 4 and suggests that as C_{Lcr} approaches C_{Lm} (i.e., as n approaches 1), cruise performance improves by virtue of

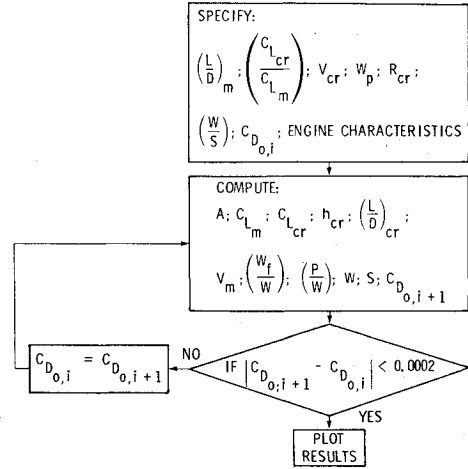


Fig. 5 Design method flow chart.

$(L/D)_{cr}$ approaching $(L/D)_m$. However, high-speed cruise near $(L/D)_m$ requires high altitudes, high wing loadings, large engines, and subsequently high gross weights. The final effect may not produce the best fuel efficiency by designing to cruise as near as possible to $(L/D)_m$. Figure 4 illustrates that increasing C_{Lcr}/C_{Lm} above about 0.7 produces diminishing returns in cruise performance. At $C_{Lcr}/C_{Lm}=0.7$, 95% of maximum (L/D) and of maximum range will be achieved.

Design Method

The principal analysis tool for matching aircraft size and weight to performance is described in Ref. 3. The basic relationships between airplane geometry and performance were programmed in a FORTRAN computer code. With the design parameters defined in Table 1, the procedure described below was used to compute airplane design tradeoff data.

In order to present data in a fashion which facilitates comparison of design points, all data are evaluated as a function of C_{Lcr}/C_{Lm} with $(L/D)_m$ held constant. Thus, while all airplanes with a given $(L/D)_m$ will have the same maximum aerodynamic cruise efficiency (i.e., the same maximum Breguet factor B), some will require less fuel for the mission by virtue of lower gross weight, smaller engine size, and lower design cruise altitudes.

The flow chart in Fig. 5 illustrates the design procedure. While the relationships used for these calculations are classical ones, they are reproduced here to clarify limitations in absolute accuracy of the results. For a specified $(L/D)_m$, the aspect ratio A required is calculated from Eq. (6) using an initial assumption for the value of C_{D0} ,

$$A = \frac{4(L/D)_m^2 C_{D0}}{\pi e} \tag{6}$$

Again, for parabolic drag polars symmetrical about zero lift,

$$C_{Lm} = \sqrt{\pi A e C_{D0}} \tag{7}$$

and with n specified, C_{Lcr} is known from Eq. (4).

With the design cruise speed V_{cr} given, cruise altitude can be determined as a function of wing loading

$$\rho_{cr} = \frac{2(W/S)}{C_{Lcr} V_{cr}^2} \tag{8}$$

Speed for maximum lift-to-drag ratio V_m can be determined from

$$V_m = \sqrt{\frac{2(W/S)}{\rho_{cr} C_{Lm}}} \tag{9}$$

For the specified cruise range R_{cr} and the Breguet factor determined from

$$B = \frac{K_3 \eta_p (L/D)_{cr}}{c} \quad (10)$$

the fuel fraction required to meet the design speed and range can be determined from the common expression

$$\frac{W_f}{W} = 1 - \frac{1}{e^{R_{cr}/B}} \quad (11)$$

Cruise power loading required is determined from

$$P_{cr}/W = (P_{cr}/P_m) (P_m/W) \quad (12)$$

where for parabolic drag polars symmetric about zero lift

$$P_{cr}/P_m = \frac{1}{2} (V_{cr}/V_m)^3 (1 + n^2) \quad (13)$$

and

$$\frac{P_m}{W} = \frac{C_{D0} (W/S)^{0.5}}{K_5 (\sqrt{\sigma}) (C_{L_m})^{1.5}}$$

With the altitude and engine lapse rate K_4 known, sea-level installed power loading is determined from

$$P_{sl}/W = (P_{cr}/W) K_4 \eta_p^{-1} \quad (14)$$

and knowing the propulsion system specific weight K_2 , the airplane useful load fraction is determined (from Ref. 3),

$$\bar{U} = -K_2 P_{sl}/W + K_1 \quad (15)$$

From Eq. (2) and $W_e = W - W_p - W_f$, gross weight can now be determined from

$$W = \frac{W_p}{\bar{U} - [W_f/W]} \quad (16)$$

At this point in the procedure (see Fig. 5), the most recent value of C_{D0} can be determined from Eq. (1), compared with the initially assumed value and convergence sought. Note that this process forces convergence to the specified value of $(L/D)_m$ by varying the aspect ratio in Eq. (6).

The computations are repeated for the range of wing loadings desired, the range of $C_{L_{cr}}/C_{L_m}$ desired, and the range of $(L/D)_m$ desired. In each case, specific range (km/l) is calculated at constant Breguet factor and constant weight (using gross weight).

Results and Discussion

Parameter values for this study were based on existing conventional propulsion, aerodynamic, and structural technologies. A set of airplane design parameters resulting from this study illustrates the potential for achieving fuel efficient, high-speed, long-range mission performance in a single-engine airplane by virtue of matching the airplane design to cruise performance requirements. The airplane design characteristics (wing geometry, engine size, etc.) which result from this analysis are not constrained by takeoff field length requirements, stall-speed requirements, climb performance requirements, or mission profile effects. It can be shown that engines which meet the cruise design requirements would be flat-rated to meet typical general aviation field length requirements. The wing loading tradeoff data generated are presented in Fig. 6 for $(L/D)_m = 14$. At any given wing loading, it can be observed that a value of $C_{L_{cr}}/C_{L_m}$ exists for which specific range is maximum. This

results from the effect discussed earlier of diminishing returns in $(L/D)_{cr}$ for increasing $C_{L_{cr}}/C_{L_m}$.

In order to compare airplane tradeoff data at varying values of $(L/D)_m$, all of the airplane characteristics which occur at the value of $C_{L_{cr}}/C_{L_m}$ for maximum specific range are crossplotted in Fig. 7. These crossplotted data present the ranges of design characteristics for the most fuel efficient airplanes at each wing loading and $(L/D)_m$ of interest.

The trends shown in Fig. 7 indicate increasing specific range with increasing $(L/D)_m$ and with increasing wing loading. Resulting cruise altitudes vary between 11,300 and 13,500 m (37,000 and 44,000 ft). Brake cruise power varies between 200 and 300 kW (250 and 400 hp). Gross weights for these designs range between 18,000 and 22,000 N (4000 and 5000 lb); while the fuel required for the mission varies between 2200 and 4000 N (500 and 900 lb). The wing areas which result vary between 6 and 16 m² (70 and 170 ft²). Finally, the aspect ratios required to achieve the specified values of $(L/D)_m$ range between 5 and 17.

At this point, it is useful to discuss the influence of practical limiting operating and geometry factors on the selection of an airplane design point. Two important parameters which have more obvious practical limits are aspect ratio and wing loading.

For the analysis of a baseline technology airplane, aspect ratios less than about 12 may be considered practical for aluminum structures. Aspect ratios greater than 12 might be practical for composite structures, however. At the other extreme, aspect ratios less than 5 may produce approach lift-to-drag ratios too low for safe approach glide-path angles for general aviation operations.

Practical values of wing loading can be judged from resulting stall speed and wing areas. Figure 8 illustrates the effect of wing loading and maximum lift coefficient on stall speeds and depicts stall speeds for current general aviation airplanes. If as an arbitrary objective, it is desired to maintain single-engine stall speeds near the values for current twins, Fig. 8 shows that wing loadings over 2400 N/m² (50 lb/ft²) may be considered reasonable. This assumes high-lift systems are incorporated to achieve maximum lift coefficients greater than 2.5.

At such high wing loadings, however, wing areas for cruise matched airplanes become small (less than 7 m², see Fig. 7). Thus fuel and landing gear volume requirements may constrain maximum practical wing loading.

A preliminary analysis was conducted of available fuel volumes in a straight tapered wing of 50% taper ratio, with fuel cells between the 15 and 65% chord locations, and with 15% wing thickness. The results indicate sufficient fuel volumes at 6.5 lb/gal exist for this mission in wings for which wing area $S \geq 7.4$ m² (80 ft²) and $A \leq 10$. Such geometry constraints limit wing loading to less than about 2630 N/m² (55 lb/ft²). Thus fuel volume appears to place practical upper limits on both wing loading and aspect ratio for the missions being analyzed.

One important benefit of higher wing loadings would be the improved ride qualities due to reduced gust response. For this very high-speed, long-range airplane, passenger comfort is an important consideration.

With these practical considerations on aspect ratio ($A \leq 10$) and wing loading ($W/S \leq 2630$ N/m²) point A on Fig. 7 may be used to illustrate a design point for a high-performance, single-engine airplane. It is seen that values of specific range near 5.9 km/l (12 n.mi./gal) might be achieved by this airplane design point. As shown below, these high levels of fuel efficiency are very attractive compared to existing airplane performance.

Figure 9 illustrates the relative merit of this cruise performance compared to existing general aviation airplanes. It can be seen that the cruise matched, high-performance, single-engine airplane concept offers the potential for a 200-400% greater fuel efficiency than current airplanes capable of

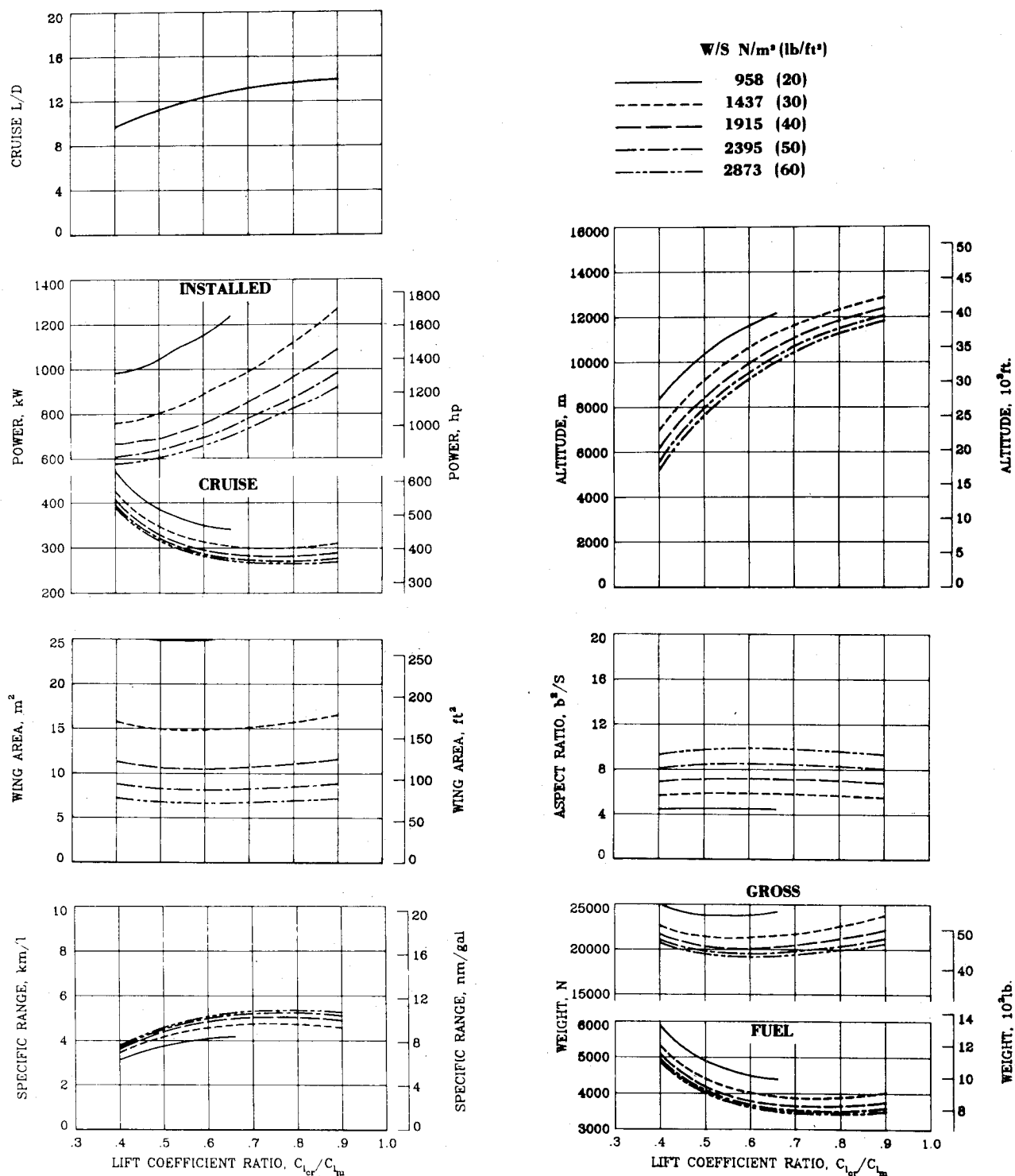


Fig. 6 Wing loading tradeoff data for a high-performance, single-engine airplane; $V_{cr} = 300$ knots; $R_{cr} = 1300$ n.mi., $W_p = 5338$ N (1200 lb), $(L/D)_m = 14$.

similar cruise speeds and payloads. Concomitantly, this cruise matching design procedure offers potential for a 50-100% greater cruise speed than current airplanes which possess approximately the same fuel efficiency (specific range). The solid symbols on Fig. 9 indicate current airplanes which, at best, have the same full fuel payloads as the design value used in this study [$W_p = 5338$ N (1200 lb)].

The benefits of the high-performance single class of airplanes, relative to the current twins, result from several factors. In addition to being aerodynamically cleaner than a twin with wing-mounted engines, the single incurs no weight or surface area penalties owing to tail sizing for engine-out

considerations. Additional weight savings accrue in engine structural support and propeller weights owing to the single vs twin configuration and power requirements. In addition, the use of the turbine engine provides benefits in propulsion system weight and cooling drag (compared to piston engines), and provides sufficient power available at high altitudes for cruise optimization.

A valid question to be raised is what benefits are lost if the airplane design is constrained to present stall-speed requirements. Although this question cannot be answered conclusively for all designs of interest, it is instructive to consider a sample case. Assuming that an airplane design

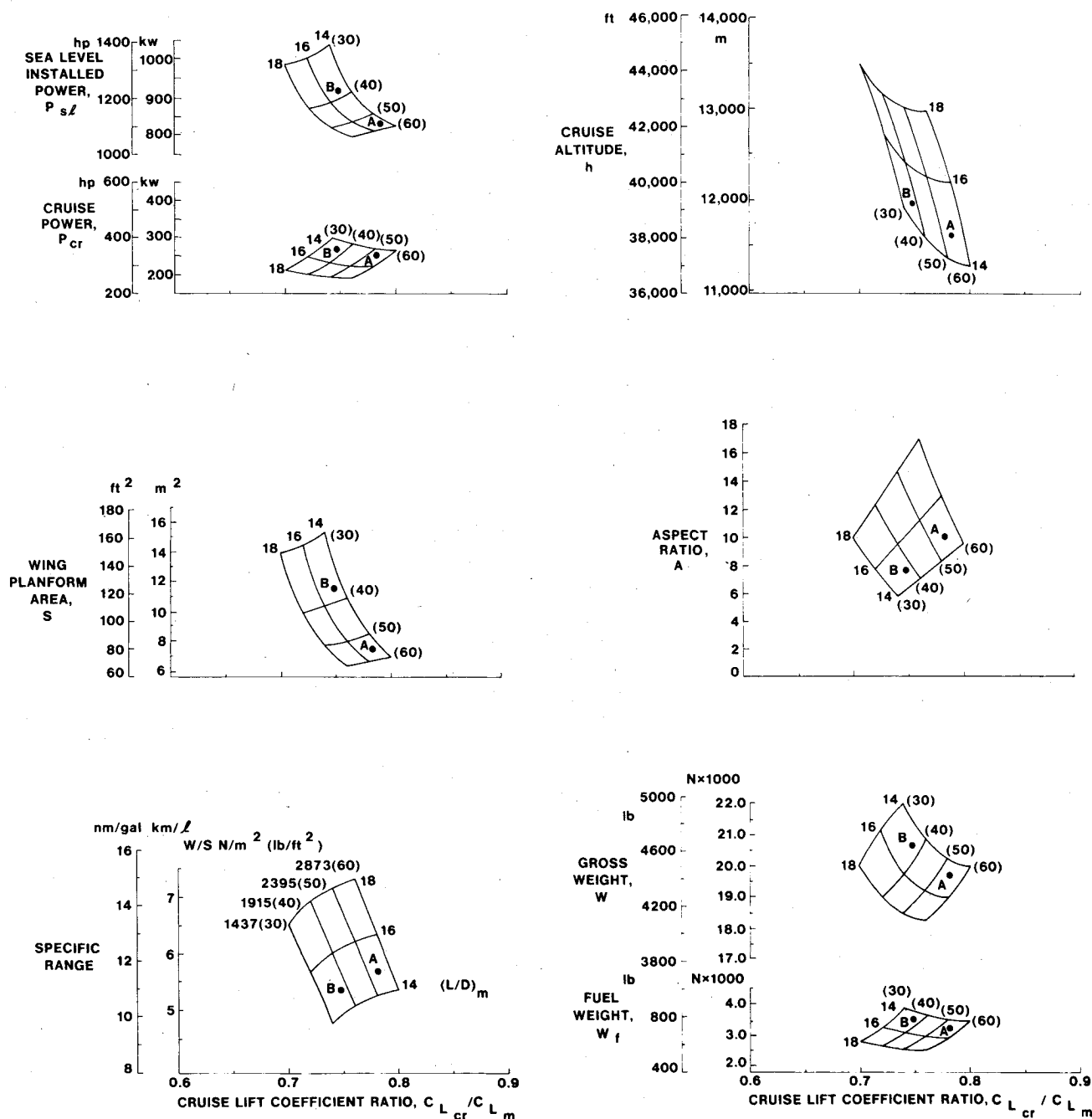


Fig. 7 Maximum fuel efficiency crossplots for high-performance, single-engine airplanes; $V_{cr} = 300$ knots, $R_{cr} = 1300$ n.mi., $W_p = 5338$ N (1200 lb). Point A: Fuel volume limited wing area and aspect ratio. Point B: Stall-speed limited wing loading at $C_{L_{max}} = 3.0$.

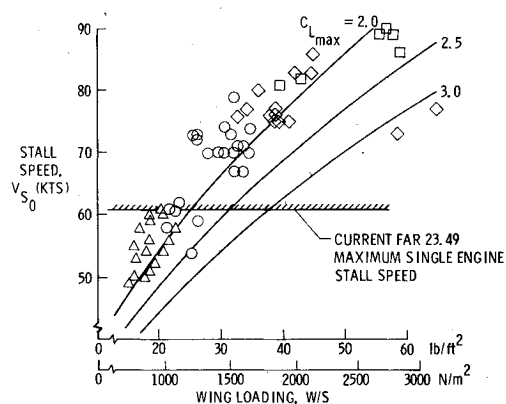


Fig. 8 Effect of wing loading and maximum lift characteristics on general aviation airplane stall speeds.⁴

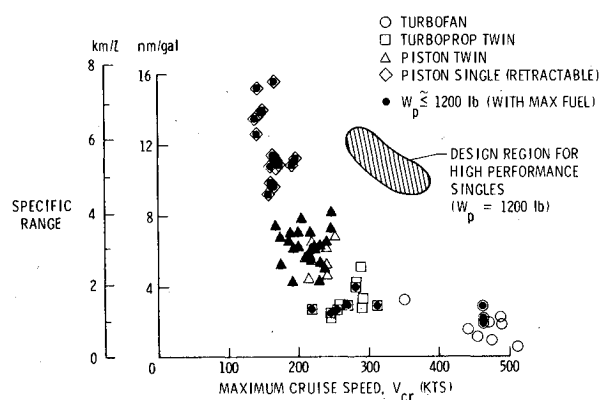


Fig. 9 Comparison of fuel efficiencies for a high-performance, single-engine airplane and current airplanes.

approached $C_{L_{\max}} \cong 3.0$, Fig. 8 shows that the maximum allowable wing loading would be about 1700 N/m^2 (38 lb/ft^2) under FAR 23 single-engine, stall-speed regulations. Point B on Fig. 7 illustrates an airplane design point which could be achieved with this wing loading constraint (assuming the same $(L/D)_m$ and, therefore, the same fuel fraction as airplane A).

Comparison of the design points A (fuel volume limited) and B (stall speed limited) on Fig. 7 can be used to estimate the penalty for designing such an airplane with the FAR 23 stall-speed constraint imposed. The difference in the total fuel required at these two design points is about 7%. However, as data on Fig. 7 illustrate, additional penalties accrue in 3% higher cruise altitude, 12% larger engine, and 5% higher gross weight owing to the smaller value for design wing loading. Thus the total penalties from constraining the design of this class of airplane to low wing loadings (i.e., low stall speeds) involve more than cruise fuel consumption. It is noteworthy, however, that even if this class of airplane is constrained by the FAR 23 stall-speed requirements, the resulting airplane designs possess desirable cruise performance characteristics.

Concluding Remarks

Design data have been presented for a class of high-performance, single-engine business airplanes. The design objectives included a cruise speed of $V_{cr} = 300$ knots, a cruise payload of six passengers with baggage, and a cruise range (no reserves) of 1300 n.mi. Existing aerodynamic, propulsion, and structural technology have been assumed for this study.

The tradeoff data presented illustrated ranges of wing loading, maximum (L/D) , and $C_{L_{cr}}/C_{L_m}$ which produce fuel efficient, cruise-matched airplane performance. It has been illustrated that wing loadings higher than presently practical (owing to existing stall-speed regulations) offer significant benefits in the design of this class of airplane. Clearly, the proposed use of high values of design wing loading for a single-engine airplane needs further discussion, especially regarding safety. Essentially, the safety discussion tends toward a debate of risks and benefits. The risks of high wing loading are associated with high approach and landing speeds; the benefits are associated with fuel efficiency and airplane performance. This is a very large debate and the present study claims only to present the benefits of cruise-matched design wing loadings. However, it may be instructional to look briefly at the origins of the present single-

engine, stall-speed regulation. The history behind the current regulation dates back to the U.S. Department of Commerce Aeronautics Branch, Aeronautics Bulletin No. 7-A, January 1, 1932. The first reference to a 70-mph stall speed is stated therein: [all airplanes must] "land at a speed not exceeding 65 mph, except that airplanes which are neither designed nor used to carry passengers shall land at a speed not exceeding 70 mph" [Sec. 76, Para. (A) (1)]. Undoubtedly, this requirement was based on operational constraints (field lengths and surfaces, for example) as well as crash survivability. However, it might be argued that technology has radically changed operational and crashworthiness aspects of airplane design in the nearly five decades since 1932. It is also noteworthy that only pilots with high skill levels would be flying the high-performance singles and a "class rating" or other such pilot certification would seem to be a logical prerequisite for the operation of such an airplane.

In light of current technology, current market requirements, and the potential benefits presented here, special consideration of stall-speed requirements for a high-performance, single-engine class of airplanes may be warranted. Such an airplane, optimized for cruise, offers the potential for 200-400% greater fuel efficiency than is achieved by current airplanes capable of similar cruise speeds, payloads, and ranges.

Acknowledgments

The author wishes to thank Laurence K. Loftin Jr., NASA Langley Research Center (retired) for his valuable assistance in this study. The contributions of Daniel W. Banks, Oliver T. Griswold, and C.P. van Dam in the preparation of this paper are gratefully acknowledged.

References

- ¹ Mechtly, E.A., "The International System of Units—Physical Constants and Conversion Factors (Second Revision)," NASA SP-7012, 1973.
- ² Hoak, D.E. et al., "USAF Stability and Control," DATCOM, Air Force Flight Dynamics Laboratory, Wright-Patterson Air Force Base, Ohio, 1980.
- ³ Loftin, L. K. Jr., "Subsonic Aircraft, Evolution and the Matching of Size to Performance," NASA RP 1060, 1980.
- ⁴ *Pilot's Operating Handbook and Airplane Flight Manuals*, published by aircraft manufacturer's for individual airplane models, 1979.

Announcement: AIAA Cumulative Index, 1980-1981

The Cumulative Index of the AIAA archival journals (*AIAA Journal*; *Journal of Aircraft*; *Journal of Energy*; *Journal of Guidance, Control, and Dynamics*; *Journal of Spacecraft and Rockets*) and the papers appearing in 1980 and 1981 volumes of the *Progress in Astronautics and Aeronautics* book series is now off press and available for sale. At \$15.00 each, copies may be obtained from the Publications Order Department, AIAA, Room 730, 1290 Avenue of the Americas, New York, New York 10104. **Remittance must accompany the order.**